DOI: 10.1002/anie.201208885

Metal–Organic Frameworks

Highly Selective Detection of Nitro Explosives by a Luminescent Metal–Organic Framework**

*Sanjog S. Nagarkar, Biplab Joarder, Abhijeet K. Chaudhari, Soumya Mukherjee, and Sujit K. Ghosh**

Dedicated to Professor Parimal K. Bharadwaj on the occasion of his 62nd birthday

Rapid and selective detection of explosives has become one of the most pressing issues concerning homeland security, military applications, forensic investigations, and mine-field analysis.[1] Nitro aromatics such as 2,4,6-trinitrotoluene (TNT), 2,4-dinitrotoluene (2,4-DNT) and 2,4,6-trinitrophenol (TNP) are common ingredients of industrial explosives and found in many unexploded land mines worldwide.[1,2] The detection of nitro aromatics present in soil and groundwater is very crucial for tracing buried and underwater explosives and for environmental monitoring near ordnance bases.[3] Current high-explosive detection methods include canines or sophisticated instruments that are expensive, complex and have portability issues during in-field use.[3] Fluorescence-based detection is gaining increasing attention owing to its high sensitivity, simplicity, short response time, and its ability to be employed both in solution and solid phase. Numerous π-electron-rich fluorescent conjugated polymers have been synthesized, and are used in the detection of trace amounts of nitro aromatics.[4]

Although extremely high sensitivity toward nitro aromatic explosives has been demonstrated, the quick and selective detection of nitro explosives is still an unexplored area. Selectivity is critical for fruitful detection in practical applications. The selective detection of TNT or TNP from a mixture by photo induced electron transfer (PET) is very difficult, as both of them have extremely strong electron affinity.[5] Targeting specific chemical and/or physical properties in addition to strong electron affinity can be a better approach for overcoming this problem. The major focus of current research is on the detection of TNT, despite the superior explosive power of TNP.[6] Also, TNP is widely used in dyes, fireworks, matches, glass, and leather industries.[7] During commercial production and use, TNP is released into the environment, leading to the contamination of soil and aquatic systems. During mammalian metabolic processes, TNP transforms into picramic acid (2-amino-4,6-dinitrophenol), which has ten times more mutagenic activity than TNP.[8] Thus, there is an urgent need for efficient and reliable sensors for TNP.

Metal organic frameworks (MOFs) are well known for their applications in molecular storage, separation, drug delivery, and catalysis.[9] Detectable changes in luminescence by tuning the host–guest chemistry along with tailorable porosity and a high surface area makes MOFs excellent candidates for sensing.[10] The use of a metal ion with a high complexation affinity and non-detrimental fluorescence connected by a luminescent ligand can be a good strategy to synthesize fluorescent MOFs.[11] The pioneering work of Li et al. and others has demonstrated the potential of luminescent MOFs in explosives detection.[12] These MOF materials exhibit fast, highly sensitive, and reversible nitro-explosives sensing. However, the selective detection of one nitro explosive in the presence of others has not been reported (Scheme 1). Herein, we report the selective detection of the nitro explosive TNP by a fluorescent metal–organic framework, $[Cd(NDC)_{0.5}(PCA)]{\cdot}G_x$ (**1**; Figure 1). For the first time, the selective detection of TNP in the presence of other nitro compounds has been demonstrated in MOFs. The selectivity for TNP is achieved by accessible basic sites, such as the amine or pyridine groups present in conjugated organic fluorophores, but no such report is known for MOF-based materials.[7,13]

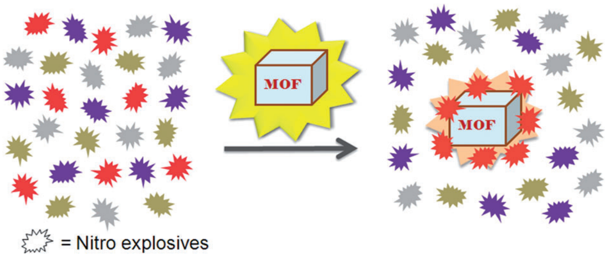

Scheme 1. MOF-based sensor for the selective detection of target nitro explosives in the presence of other nitro compounds.

A luminescent 3D porous MOF, $[Cd(NDC)_{0.5}(PCA)]{\cdot}G_x$ (**1**; G = guest molecules, NDC = 2,6-napthalenedicarboxylic acid, PCA = 4-pyridinecaboxylic acid), was synthesized using Cd^{2+} and luminescent NDC and PCA ligands. Compound **1** has a 1D channel (ca. 9.48×7.83 Å^2) along the c axis that is occupied with solvent molecules. The channels are lined with

---

[*] S. S. Nagarkar, B. Joarder, A. K. Chaudhari, S. Mukherjee, Dr. S. K. Ghosh
Indian Institute of Science Education and Research (IISER)
Dr. Homi Bhabha Road, Pashan, Pune-411008 (India)
E-mail: sghosh@iiserpune.ac.in
Homepage: http://www.iiserpune.ac.in/~sghosh/

[**] We are grateful to IISER Pune and DST (GAP/DST/CHE-12-0083) for financial support. We also thank HEMRL, Pune for TNT and RDX samples. We acknowledge Dr. Partha Hazra and group for valuable discussions during our fluorescence studies.

Supporting information for this article is available on the WWW under http://dx.doi.org/10.1002/anie.201208885.

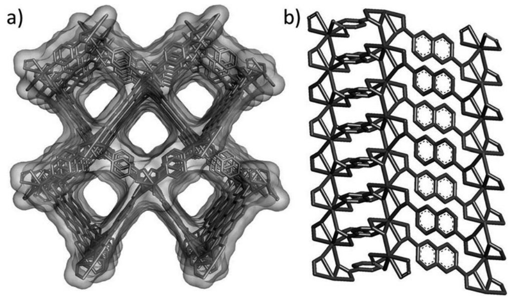

Figure 1. a) 3D porous framework of **1** along the *c* axis, b) 1D channel lined with naphthalene moieties along the *b* axis. Guest molecules and hydrogen atoms are removed for clarity.

the π-electron-rich naphthalene moiety of NDC, whereas the aromatic rings from the PCA ligands are perpendicular to the channel wall. The guest molecules can be removed by exchanging **1** with MeCN followed by heating to get the guest-free form, **1′**. The structure remains intact upon guest removal and remains stable even in presence of water vapor. PLATON analysis revealed that the 3D porous structure is composed of large solvent-accessible voids of 1505.2 Å^3 that constitute 34.9% volume per unit cell.[14] The porosity was also confirmed by CO_2 and benzene sorption analysis at 195 K and 298 K, respectively (Figures S1 and S2).

The photoluminescence (PL) spectrum of **1′** dispersed in MeCN exhibits strong emission at 384 nm when excited at 340 nm (Figure S3). To explore the ability of **1′** to sense a trace quantity of nitro explosives, fluorescence-quenching titrations were performed with the incremental addition of analytes to **1′** dispersed in MeCN. Fast and high fluorescence quenching was observed upon incremental addition of a TNP solution (1 mM). The visible bright blue emission of **1′** in UV light vanished upon the addition of the TNP solution, which quenched nearly 78% of the initial fluorescence intensity (Figures 2 and 3a). The fluorescence quenching by TNP could be easily discerned at low concentration (4 μM; Figure S4).

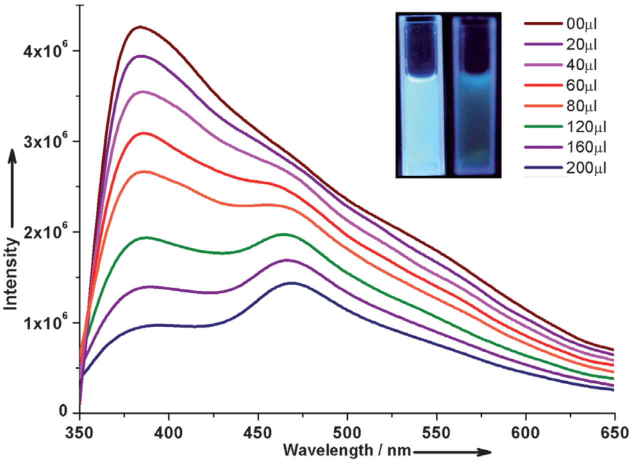

Figure 2. Effect on the emission spectra of **1′** dispersed in MeCN upon incremental addition of a TNP solution. Inset: a photograph showing the original fluorescence and the decreased fluorescence upon addition of TNP.

Fluorescence quenching titrations were also performed with nitro aromatics such as TNT, 2,4-DNT, 2,6-dinitrotoluene (2,6-DNT), 1,3-dinitrobenzene (DNB), nitrobenzene (NB), and nitro-aliphatic compounds such as 2,3-dimethyl-2,3-dinitrobutane (DMNB), nitromethane (NM), and 1,3,5-trinitro-1,3,5-triazacyclohexane (nitro-amine RDX). All other nitro compounds showed little effect on the fluorescence intensity (Figures 3a, and S5–S12). These results demonstrate

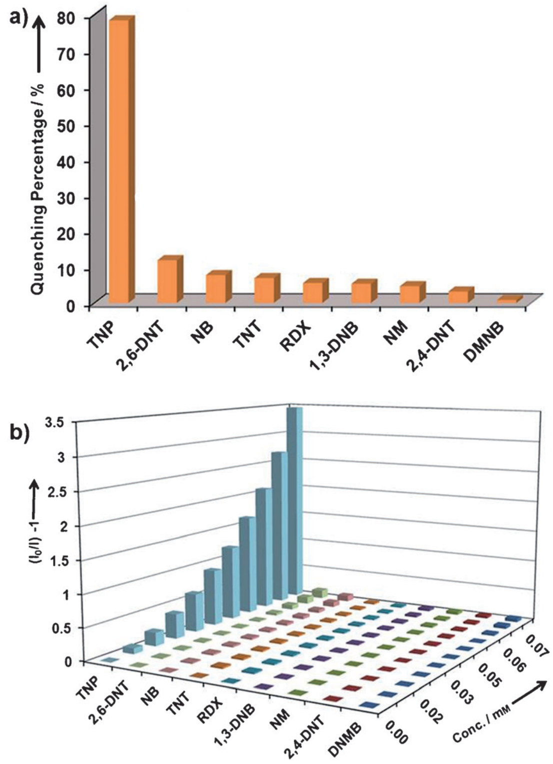

Figure 3. a) Percentage of fluorescence quenching obtained for different analytes at room temperature. b) Corresponding Stern–Volmer plots of analytes.

that compound **1′** has high selectivity for TNP compared to other nitro compounds. The powder X-ray diffraction (PXRD) patterns of compound **1′** showed that the compound remains stable, even after fluorescence titrations with different analytes (Figure S13). Further, the fluorescence quenching efficiency was analyzed using the Stern–Volmer (SV) equation, $(I_0/I) = K_{sv}\,[A] + 1$, where I_0 is the initial fluorescence intensity before the addition of analyte, I is the fluorescence intensity in the presence of analyte, $[A]$ is the molar concentration of analyte, and K_{sv} is the quenching constant (M^{-1}). The SV plot for TNP was nearly linear at low concentrations and subsequently deviated from linearity, bending upwards at higher concentrations. The nonlinear nature of the SV plot of TNP can be ascribed to a self-absorption or energy transfer process.[1a,15] All the other nitro compounds showed linear SV plots (Figure 3b). The quenching constant for TNP was found to be $3.5 \times 10^4\,\mathrm{M}^{-1}$, which is comparable to known organic polymers.[16] The quenching constant for TNP is ca. 30 times greater than for TNT and

RDX, which is the highest value known for MOF-based sensors indicating an excellent quenching efficiency towards luminescent **1′**.

The selective detection of TNP in an aquatic system is highly desirable for practical applications. To study the selective detection of TNP from aqueous samples, the fluorescence response of **1′** (in MeCN) upon addition of water was initially monitored. The water showed a negligible effect on fluorescence intensity and the spectrum remains unaffected even after 1 h (Figure S14). The PXRD patterns before and after the addition of water demonstrates the stability of **1′** towards water (Figure S15). Interestingly the addition of an aqueous solution of TNP (1 mM) to **1′** (in MeCN) also resulted in a fast and high (78 %) fluorescence quenching response (Figure S16). Motivated by these results, we thought to check the selectivity for TNP in the presence of other nitro compounds. In a specially designed experiment, the fluorescence spectrum for **1′** dispersed in MeCN was recorded, to this was added a saturated aqueous solution of TNT followed by TNP (1 mM) and the corresponding emissions were monitored. The TNT was added initially, so that high affinity binding sites will be accessible to TNT, but the addition of TNT showed very little effect on fluorescence intensity. On the other hand, the addition of an aqueous solution of TNP to a TNT-containing solution, gave significant fluorescence quenching, with the quenching efficiency of TNP remaining unaffected, even through further addition sequences (Figure S17). The addition of saturated aqueous solutions of other nitro compounds also showed negligible effect on the fluorescence intensity, whereas aqueous TNP quenched the fluorescence effectively (Figure S18–S24). Similar results were obtained upon addition of MeCN solutions of nitro compounds followed by TNP to **1′** (Figure S25–32). The results can be easily visualized by plotting the percentage fluorescence intensity versus volume of analyte added (Figure 4). The stepwise decrease in fluorescence intensity clearly demonstrates the unprecedented selectivity of **1′** for TNP, even in the presence of a higher concentration of other nitro compounds. Species **1′** outperforms previously reported TNP chemo sensors, which are highly sensitive, but suffer interference from other electron-deficient compounds. The highly selective detection in an aqueous sample in the presence of other nitro compounds makes **1′** a reliable sensor for TNP.[7]

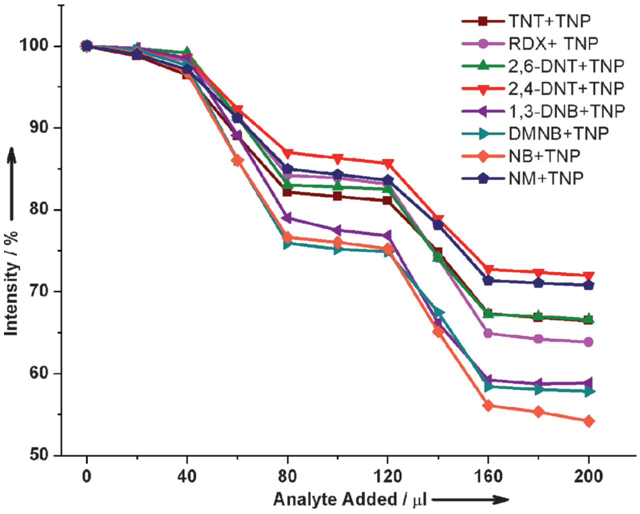

Figure 4. Decrease in percentage of fluorescence intensity upon the addition of aqueous solutions of different nitro compounds followed by TNP.

To understand the origin of the high selectivity of **1′** towards TNP, the mechanism of quenching was investigated. Owing to pore size limitations, only surface adsorption occurs for nitro compounds, except in the case of NM. The MOFs, especially with d^{10} metal ions, can be regarded as giant "molecules" and their valence and conduction bands can be treated in a fashion similar to molecular orbitals (MOs).[12b] Generally, the conduction band of a MOF lies at higher energies than the LUMOs of analytes, and thus maintains a better driving force for electron transfer to electron-deficient analytes, thus resulting in fluorescence quenching. Figure 5 shows the HOMO and LUMO orbital energies of electron-deficient nitro compounds, as calculated by density functional theory at the B3LYP/6-31G* level (Table S2). These LUMO energy levels, which are arranged in descending energy order, are expected to represent how easily an electron can be transferred to the electron-deficient analyte in the fluorescence quenching process.[2,16b] The LUMO energies were in good agreement with the maximum quenching observed for TNP, but the order of observed quenching efficiency is not fully in accordance with the LUMO energies of other nitro compounds. This indicates that the photo-induced electron transfer is not the only mechanism for quenching.

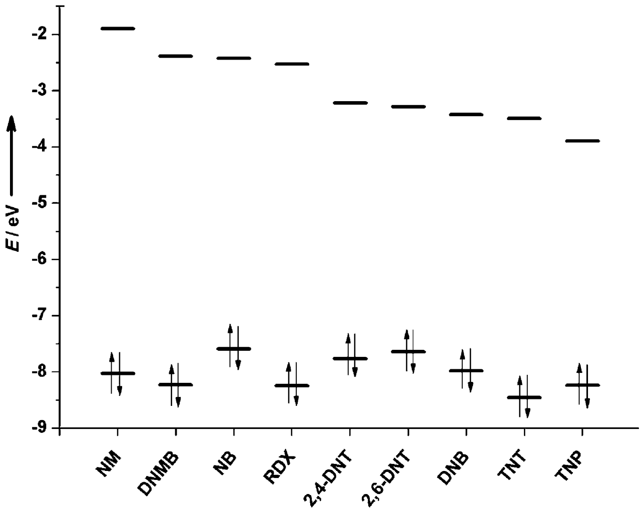

Figure 5. HOMO and LUMO energies for explosive analytes arranged in descending order of LUMO energies.

The non-linear S–V plot for TNP suggests an energy transfer mechanism. The resonance energy transfer can occur from fluorophore to non-emissive analyte, if the fluorophore and analyte are close to each other and the absorption band of the analyte has an effective overlap with the emission band of the fluorophore. Resonance energy transfer can dramatically enhance fluorescence-quenching efficiency and also improves sensitivity.[17] The probability of resonance energy transfer depends upon the extent of spectral overlap between the absorption band of the analyte and the emission band of the fluorophore. Figure 6 shows that the absorption spectrum of TNP has a large overlap with the emission spectrum of **1′**, whereas almost no overlap was observed for RDX, DMNB, NM, or other nitro aromatics. The extent of energy transfer was determined by calculating the integral of overlap (J_λ) values using Equation (1).[18] Where, $F_D(\lambda)$ is the corrected fluorescence intensity of donor in the range of λ to $\lambda+\Delta\lambda$ with the total intensity normalized to unity, and ε_A is extinction coefficient of the acceptor at λ in $\mathrm{M^{-1}cm^{-1}}$. The highest J_λ value was observed for TNP ($1.39\times10^{14}\,\mathrm{M^{-1}cm^{-1}nm^4}$), which was almost ten times more than NB, 2,4-DNT, and 1,3-DNB, and 100 times more than for TNT, RDX, 2,6-DNT, NM, and DMNB. The presence of energy transfer was also supported by the preferential quenching of the 384 nm peak over 470 nm in Figures 2 and S16. The peak at 384 nm has a spectral overlap with the absorption spectrum of TNP, so the efficient quenching of this peak occurs by an energy transfer mechanism, which leads to a higher quenching response. On the other hand, the peak at 470 nm has no overlap with the absorption spectrum of TNP (Figure 6), so the quenching occurs by an electron transfer mechanism and thus a small quenching response towards TNP is observed. This result establishes that both energy transfer and electron transfer mechanisms are present, and that the energy transfer mechanism is predominant over the electron transfer mechanism in fluorescence quenching by TNP. For other nitro compounds, the quenching occurs only by electron transfer. The energy transfer is a long-range process, thus emission quenching by TNP is carried over the surrounding fluorophores, thus amplifying the quenching response of **1′**. On the other hand, electron transfer is a short-range process, so the emission quenching by other nitro compounds is limited to the fluorophores that have direct interaction with the analyte. Thus, **1′** responds more selectively to TNP than to other nitro compounds.

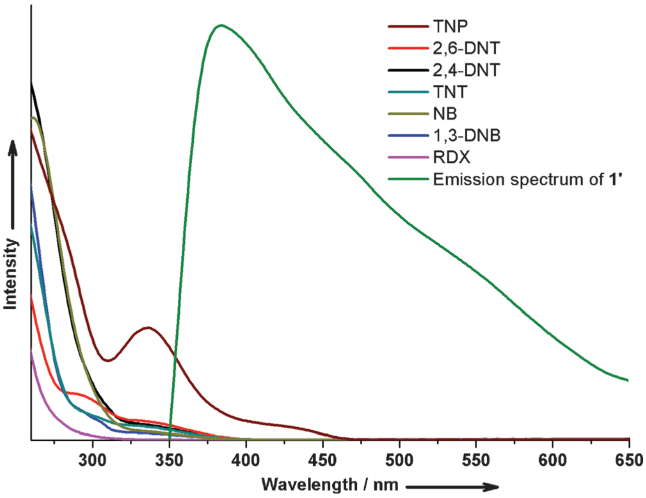

Figure 6. Spectral overlap between the absorption spectra of analytes and the emission spectrum of **1′** in MeCN.

$$J(\lambda) = \int_0^\infty F_D(\lambda)\varepsilon_A(\lambda)\lambda^4 \mathrm{d}\lambda \qquad (1)$$

Species **1′** has an unsaturated pyridine nitrogen on the surface; so, to trace presence of electrostatic interactions that can lead to the special selectivity of **1′** for TNP, fluorescence-quenching titrations were performed with 4-nitrophenol (NP) and 2,4-dinitrophenol (2,4-DNP; Figure S33, S34). The order of the quenching efficiency was found to be TNP ≫ 2,4-DNP > NP, which is in complete agreement with the order of acidity of these analytes (TNP ≫ 2,4-DNP > NP; Figure S35). This may explain the unprecedented selectivity for TNP, as other nitro compounds do not have a hydroxy group and so they cannot interact strongly with the free basic sites of the fluorophore (pyridine nitrogen on the surface) and so result in a very low quenching effect. On the other hand, hydroxy-group-containing analytes such as TNP, 2,4-DNP, NP can interact with the basic sites of **1′**, and do so in the order of their acidity. TNP, with its highly acidic hydroxy group interact strongly with the fluorophore and the quenching effect is carried over long range owing to the energy transfer mechanism, thus leading to an amplified response. So, compared to other nitro compounds, species **1′** exhibits a much higher fluorescence quenching response towards TNP, owing to favorable electron and energy transfer mechanisms, as well as electrostatic interactions. Thus, the presence of free basic sites in MOFs can be a useful tool to achieve the selective detection of TNP over other nitro compounds.

In conclusion, a 3D fluorescent metal–organic framework for the highly selective detection of the nitro explosive TNP has been reported. The compound exhibited selective detection of TNP, even in the presence of other nitro compounds in both aqueous and organic solution. The selectivity is ascribed to electron and energy transfer mechanisms, as well as electrostatic interactions between TNP and the fluorophore. Despite the limited water stability and the toxicity of the reported $\mathrm{Cd^{II}}$ MOF, our results demonstrate a promising approach to achieve highly selective TNP sensing in MOFs. Thus, the luminescent porous MOFs with high water stability, large spectral overlap, and electrostatic interactions with TNP, could be promising candidates for practical TNP sensing.[17c] Finally, the present study provides a new insight into the design of MOF-based explosive sensors, which are likely to be useful under more realistic conditions in the near future.

Received: November 6, 2012
Revised: December 17, 2012

Keywords: explosives · fluorescence · metal-organic frameworks · sensors

---

[1] a) Y. Salinas, R. Martinez-Manez, M. D. Marcos, F. Sancenon, A. M. Castero, M. Parra, S. Gil, *Chem. Soc. Rev.* **2012**, *41*, 1261 –

1296; b) S. W. Thomas III, G. D. Joly, T. M. Swager, *Chem. Soc. Rev.* **2007**, *36*, 1339–1386.

[2] M. E. Germain, M. J. Knapp, *Chem. Soc. Rev.* **2009**, *38*, 2543–2555.

[3] a) H. Sohn, M. J. Sailor, D. Magde, W. C. Trogler, *J. Am. Chem. Soc.* **2003**, *125*, 3821–3830.

[4] a) M. E. Germain, M. J. Knapp, *J. Am. Chem. Soc.* **2008**, *130*, 5422–5423; b) Y. Che, D. E. Gross, H. Huang, D. Yang, X. Yang, E. Discekici, Z. Xue, H. Zhao, J. S. Moore, L. Zang, *J. Am. Chem. Soc.* **2012**, *134*, 4978–4982; c) K. K. Kartha, S. S. Babu, S. Srinivasan, A. Ajayaghosh, *J. Am. Chem. Soc.* **2012**, *134*, 4834–4841; d) R. Li, Y.-P. Yuan, L.-G. Qui, W. Zhang, J.-F. Zhu, *Small* **2012**, *8*, 225–230; e) Y. Wang, A. La, Y. Ding, Y. Liu, Y. Lei, *Adv. Funct. Mater*, **2012**, *22*, 3547–3555.

[5] B. Xu, X. Wu, H. Li, H. Tong, L. Wang, *Macromolecules* **2011**, *44*, 5089–5092.

[6] N. Venkatramaiah, S. Kumar, S. Patil, *Chem. Commun.* **2012**, *48*, 5007–5009.

[7] G. He, H. Peng, T. Liu, M. Yang, Y. Zhang, Y. Fang, *J. Mater. Chem.* **2009**, *19*, 7347–7353.

[8] a) P. G. Thorne, T. F. Jenkins, *Field Anal. Chem. Technol.* **1997**, *1*, 165–170; b) K. M. Wollin, H. H. Dieter, *Arch. Environ. Contam. Toxicol.* **2005**, *49*, 18–26.

[9] a) R. Kitaura, S. Noro, S. Kitagawa, *Angew. Chem.* **2004**, *116*, 2388–2430; *Angew. Chem. Int. Ed.* **2004**, *43*, 2334–2375; b) J. J. Vittal, *Coord. Chem. Rev.* **2007**, *251*, 1781–1795; c) G. Férey, C. Serre, *Chem. Soc. Rev.* **2009**, *38*, 1380–1399; d) X. N. Cheng, W. X. Zhang, Y.-Y. Lin, Y. Z. Zheng, X.-M. Chen, *Adv. Mater.* **2007**, *19*, 1494–1498; e) J. An, S. J. Geib, N. L. Rosi, *J. Am. Chem. Soc.* **2009**, *131*, 8376–8377; f) B. Zheng, J. Bai, J. Duan, L. Wojtas, M. J. Zawototko, *J. Am. Chem. Soc.* **2011**, *133*, 748–751; g) S. T. Zheng, J. T. Bu, Y. Li, T. Wu, F. Zuo, P. Feng, X. Bu, *J. Am. Chem. Soc.* **2010**, *132*, 17062–17064; h) M. Banerjee, S. Das, M. Yoon, H. J. Choi, M. H. Hyun, S. M. Park, G. Seo, K. Kim, *J. Am. Chem. Soc.* **2009**, *131*, 7524–7525; i) A. K. Cheetham, C. N. R. Rao, *Science* **2007**, *318*, 58–59; j) H.-C. Zhou, J. R. Long, O. M. Yaghi, *Chem. Rev.* **2012**, *112*, 673–674, and references therein; k) M. D. Allendorf, C. A. Bauer, R. K. Bhakta, J. T. Houk, *Chem. Soc. Rev.* **2009**, *38*, 1330–1352; l) I. Senkovska, F. Hoffman, M. Froba, J. Getzschmann, W. Bohlmann, S. Kaskel, *Microporous Mesoporous Mater.* **2009**, *122*, 93–98.

[10] K. C. Stylianou, R. Heck, S. Y. Chong, J. Bacsa, J. T. A. Jones, Y. Z. Khimyak, D. Bradshaw, M. J. Rosseinsky, *J. Am. Chem. Soc.* **2010**, *132*, 4119–4130.

[11] L. E. Kreno, K. Leong, O. K. Farah, M. Allendorf, R. P. Van Duyne, J. T. Hupp, *Chem. Rev.* **2012**, *112*, 1105–1125.

[12] a) A. Lan, K. Li, H. Wu, D. H. Olson, T. J. Emge, W. Ki, M. Hong, J. Li, *Angew. Chem.* **2009**, *121*, 2370–2374; *Angew. Chem. Int. Ed.* **2009**, *48*, 2334–2338; b) S. Pramanik, C. Zheng, X. Zhang, T. J. Emge, J. Li, *J. Am. Chem. Soc.* **2011**, *133*, 4153–4155; c) H. L. Jiang, Y. Tatsu, Z. H. Lu, Q. Xu, *J. Am. Chem. Soc.* **2010**, *132*, 5586–5587; d) S. Das, P. K. Bharadwaj, *Inorg. Chem.* **2006**, *45*, 5257–5259; e) Z. Zhang, S. Xiang, X. Rao, Q. Zheng, F. R. Fronczek, G. Qian, B. Chen, *Chem. Commun.* **2010**, *46*, 7205–7207; f) H. Xu, F. Liu, Y. Cui, B. Chen, G. Qian, *Chem. Commun.* **2011**, *47*, 3153–3155; g) C. Zhang, Y. Che, Z. Zhang, X. Yang, L. Zang, *Chem. Commun.* **2011**, *47*, 2336–2338; h) B. Gole, A. K. Bar, P. S. Mukherjee, *Chem. Commun.* **2011**, *47*, 12137–12139; i) C. Wang, W. Lin, *J. Am. Chem. Soc.* **2011**, *133*, 4232–4235.

[13] a) Y. Peng, A. J. Zhang, M. Dong, Y. W. Wang, *Chem. Commun.* **2011**, *47*, 4505–4507; b) Y. Zhang, Y. Guo, Y. H. Joo, D. A. Parrish, J. M. Shreeve, *Chem. Eur. J.* **2010**, *16*, 10778–10784.

[14] S. S. Nagarkar, A. K. Chaudhari, S. K. Ghosh, *Inorg. Chem.* **2012**, *51*, 572–576.

[15] a) D. Zhao, T. M. Swager, *Macromolecules* **2005**, *38*, 9377–9384; b) W. Wu, S. Ye, G. Yu, Y. Liu, J. Qin, Z. Li, *Macromol. Rapid Commun.* **2012**, *33*, 164–171.

[16] a) A. Saxena, M. Fujiki, R. Rai, G. Kwak, *Chem. Mater.* **2005**, *17*, 2181–2185; b) J. C. Sanchez, A. G. DiPasquale, A. L. Rheingold, W. C. Trogler, *Chem. Mater.* **2007**, *19*, 6459–6470.

[17] a) J. Wang, J. Mei, W. Yuan, P. Lu, A. Qin, J. Sun, Y. Ma, B. Z. Tang, *J. Mater. Chem.* **2011**, *21*, 4056–4059; b) W. Wei, X. Huang, K. Chen, Y. Tao, X. Tang, *RSC Adv.* **2012**, *2*, 3765–3771; c) S. Ramachandra, Z. D. Popovic, K. S. Schuermann, F. Cucinotta, G. Calzaferri, L. D. Cola, *Small* **2011**, *7*, 1488–1494.

[18] J. R. Lakowicz, *Principles of Florescence spectroscopy*, 3rd ed., Springer, Singapore, **2010**, pp. 443–472.